European Journal of Medicinal Chemistry 61 (2013) 95–103

Contents lists available at SciVerse ScienceDirect

European Journal of Medicinal Chemistry

journal homepage: http://www.elsevier.com/locate/ejmech

Original article

Design, synthesis and biological evaluation of benzothiazepinones (BTZs) as novel non-ATP competitive inhibitors of glycogen synthase kinase-3β (GSK-3β)

Peng Zhang [a], Hai-Rong Hu [b], Shi-Hui Bian [a], Zhao-Hui Huang [a], Yong Chu [a,*], De-Yong Ye [a,*]

[a] Department of Medicinal Chemistry, School of Pharmacy, Fudan University, 826 Zhangheng Rd, Shanghai 201203, China
[b] Key Laboratory of State Genetics Engineering, School of Life Sciences, Fudan University, 220 Handan Rd, Shanghai 200433, China

ARTICLE INFO

Article history:
Received 1 March 2012
Received in revised form
31 July 2012
Accepted 13 September 2012
Available online 21 September 2012

Keywords:
GSK-3β
Kinase inhibitor
Non-ATP competitive
Benzothiazepinones
Selectivity
Docking

ABSTRACT

Glycogen synthase kinase-3β (GSK-3β) plays a key role in type II diabetes and Alzheimer's diseases, to which non-ATP competitive inhibitors represent an effectively therapeutical approach due to their good specificity. Herein, a series of small molecules benzothiazepinones (BTZs) as novel non-ATP competitive inhibitors of GSK-3β have been designed and synthesized. The *in vitro* evaluation performed by luminescent assay showed most BTZ derivatives have inhibitory effects in micromolar scale. Among them compounds **6l**, **6t** and **6v** have the IC_{50} values of 25.0 μM, 27.8 μM and 23.0 μM, respectively. Moreover **6v** is devoid of any inhibitory activity in the assays to other thirteen protein kinases. Besides, SAR is analyzed and a hypothetical enzymatic binding mode is proposed by molecular docking study, which would be useful for new candidates design.

1. Introduction

Glycogen synthase kinase-3β (GSK-3β) plays a key role in the regulation of many physiological responses in mammalian cells as a multifunctional serine/threonine protein kinase [1]. Its phosphorylation process controls a multitude of cellular processes, including gene transcription, metabolic pathways, cell growth and differentiation, as well as apoptosis [2,3]. Thus, inhibition of GSK-3β may represent a novel approach for the therapy of several human diseases, such as type II diabetes, Alzheimer's diseases (AD), chronic inflammatory diseases, bipolar disorders and cancer [4–6].

The search for GSK-3β inhibitors has spanned more than a decade, and a number of structural diverse molecules that inhibit GSK-3β have already been reported in literature [7]. However, the great majority of them might offer unfavorable off-target effects considering they are almost ATP competitors. Such inhibitors bind competitively at the ATP binding site of GSK-3β and are likely to act on other undesirable protein kinases because of the highly conservation of ATP binding domain among more than 500 protein kinases of human kinome [8]. Nowadays non-ATP competitive inhibitors are expected to be promising drugs for reducing adverse effects. Normally these inhibitors would be inherently more specific and usually show a far better true efficacy in cell or *in vivo* assays than *in vitro* assays [9]. Thus, developing non-ATP competitive GSK-3β inhibitors with high selectivity has already been a new hot spot for medicinal chemists in recent years.

To our best knowledge, five kinds of chemical families of GSK-3β inhibitor with non-ATP competitive mechanism are already reported (see Fig. 1). It is worth noting that all of their IC_{50} values are in micromolar level, suggesting poor activity *in vitro* of such type of inhibitors. The first ones are the thiadiazolidinones (TDZDs) [10]. Among them, one compound called tideglusib (NP-12) is currently undergoing Phase IIb clinical trials both on AD and orphan tauopathy, and it is also the only GSK-3β inhibitor under clinical phase so far [11]. Halomethylketones (HMKs) are the second ones and have recently been viewed as the first irreversible GSK-3β inhibitors [12,13]. The irreversible inhibition is due to the formation of an irreversible covalent sulfur–carbon bond between the HMK moiety and the amino acid residue Cys199. This key amino acid residue plays the role as 'gatekeeper' of GSK-3β [14]. The small peptide L803-mts acts as substrate competitive inhibitor effectively *in vivo* for neurological diseases and type II diabetes [15]. Lately, two marine natural products of alkaloid manzamine A and sesterterpene palinurin are reported to well decrease tau phosphorylation as cell permeable non-ATP competitive inhibitors [5,16].

* Corresponding authors.
E-mail addresses: cy110@fudan.edu.cn (Y. Chu), dyye@shmu.edu.cn (D.-Y. Ye).

0223-5234/$ – see front matter © 2012 Elsevier Masson SAS. All rights reserved.
http://dx.doi.org/10.1016/j.ejmech.2012.09.021

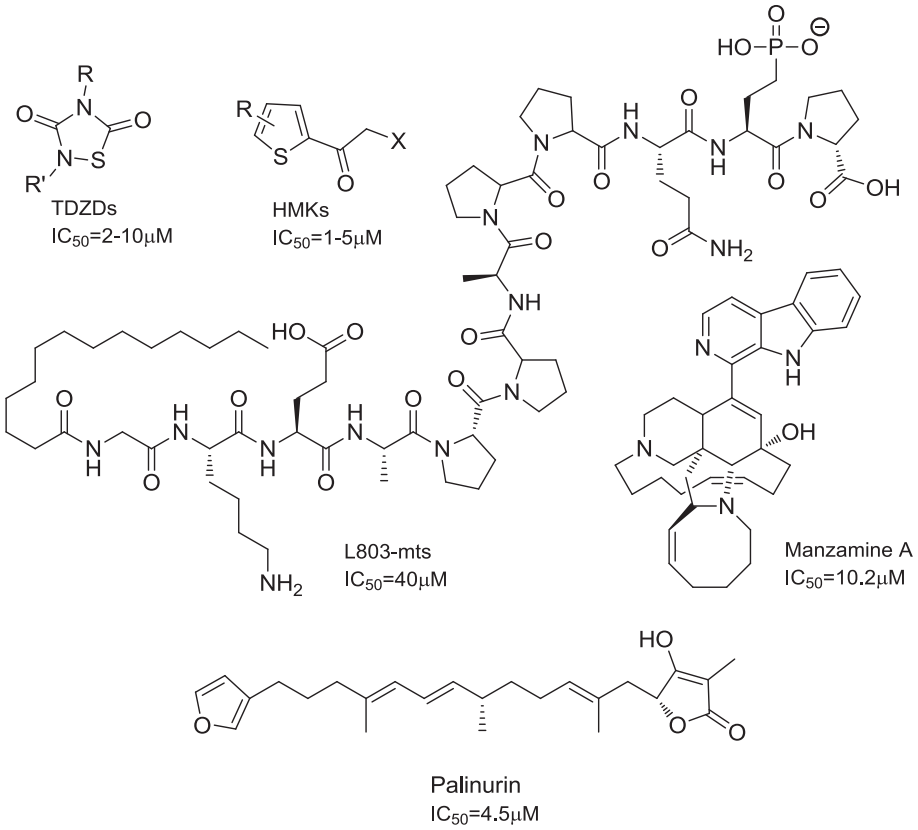

Fig. 1. Structures of reported non-ATP competitive GSK-3β inhibitors.

Herein, we report another novel small heterocyclic benzothiazepinones (BTZs) as reversible non-ATP competitive inhibitors against GSK-3β. This scaffold was found by us through a virtual screening for Maybridge database with Autodock 3.0.5. In this docking approach, the X-ray crystal structure of GSK-3β kinase (PDB ID: 1UV5) was chosen as the model of receptor and a 3D non-ATP binding pocket composed of Arg 96, Lys 205 and Tyr 216 was carefully constructed as screening receptor model. In the results several BTZ compounds were top ranked as the effective hits, and two of them were finally proved against GSK-3β with IC_{50} values of 830 μM and 480 μM respectively (Fig. 2). Inspired by its novel scaffold, more new BTZ derivatives were designed and successfully synthesized for screening of potent candidates. Finally, some of them demonstrated an *in vitro* inhibition to GSK-3β in micromolar range, and moreover the compound tested for specificity showed no activity to a panel of other 13 protein kinases, even the closest Cdk-1/cyclin B and CK-II. In this paper, the synthesis, biological evaluation and *in silico* studies, together with a preliminary structure–activity relationship (SAR) analysis will be described. The results support that the BTZ derivatives would be promising candidates for further development of pharmacotherapy.

2. Results and discussion

2.1. Chemistry

Compounds **6a**–**6y** were synthesized following the general route described in Scheme 1.

The synthesis of 3-substituted-acrylic acids **4a**–**4j** was performed by the Knoevenagel condensation of various aromatic formaldehyde **3a**–**3j** with propanedioic acid in the presence of pyridine and piperidine under reflux condition. Followed by the cyclization of resulting acids **4a**–**4j** with 2-aminobenzenethiol in high temperature without any solvent, the key intermediates of 2,3-dihydro-1,5-benzothiazepin-4(5*H*)-one analogs **5a**–**5j** were successfully obtained in moderate yields from recrystallization [17].

Through the electrophilic substitution of alkyl or acyl halides in the presence of NaH at −10 °C for 30 min, various groups, such as alkyl, aromatic alkyl or acyl were introduced to the 5-position of the BTZ framework to obtain the analogs **6a**–**6r**, **6u**–**6y**. It is worth noting that unfavorably attacking of *C*3 position could be avoided in this reaction condition [18]. As the results, the yields could be high to a range of 80%–100%.

Hydrolysis of compound **6m** was carried out in a sealed tube with concentrated hydrochloric acid at 100 °C to give compound **6s** [19], which was then treated with thionyl chloride in methanol under reflux condition to afford the corresponding methyl ester **6t** (Scheme 2).

The structures of all the new compounds are elucidated from their analytical and spectroscopic data (^1H, ^{13}C NMR and MS) which are collected in the Experimental Section.

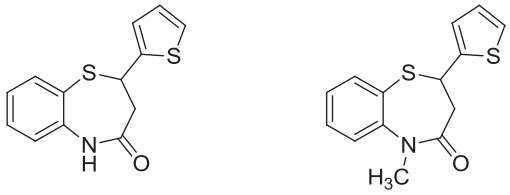

Fig. 2. Hits of 2,3-dihydro-1,5-benzothiazepin-4(5*H*)-ones from virtual screening.

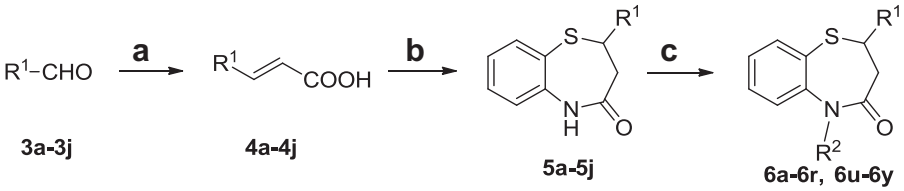

Scheme 1. (a) $CH_2(COOH)_2$, pyridine, piperidine, 2 h, reflux; (b) 2-aminobenzenethiol, 4 Å molecular sieve, 6 h, 180 °C; (c) R^2X, X = Cl or Br or I, NaH, DMF, 0.5 h, −10 °C.

2.2. Biological evaluation and SAR study

2.2.1. GSK-3β inhibition

All the newly prepared BTZ derivatives were evaluated for their GSK-3β inhibitory activity by a recently well described Kinase-Glo™ luminescent technique, which is regarded as a safer nonradioactive assay [20]. GS-2 is the most utilized substrate of GSK-3β as a small peptide similar to skeletal muscle glycogen synthase. It is composed of 26-amino acids and contains a prephosphorylated serine residue. In our assay, we used the prephosphorylated 12-amino acids polypeptide substrate ^{650}HSSPHQ (pS)EDEEE, which is as same as the one used by Andrea Baki in a high throughput luminescent assay for looking for GSK-3β inhibitors [20]. Briefly, GSK-3β enzyme was incubated with ATP and GS-2 in the presence or absence of the tested compound, and then the amount of ATP remaining in solution, which inversely correlates to kinase activity, was quantified following the kinase reaction. The IC_{50} values are listed in Table 1 and it can be seen that some of compounds really inhibit GSK-3β in micromolar scale. Among them the best three compounds **6l**, **6t** and **6v** have the IC_{50} values of 25.0 μM, 27.8 μM and 23.0 μM, respectively.

2.2.2. Mode of inhibition

In order to explore the biological mechanism of BTZ derivatives, compound **6v** was used to study the kinetic features. We firstly tested whether a competition effect exists between **6v** and ATP. That is, keeping the concentration of GS-2 unchanged, the enzyme inhibitory activities of compound **6v** were measured at its two different concentrations separately while ATP concentrations varied. The results are showed in Fig. 3A and it can be seen from the double reciprocal plotting of the data, in which compound **6v** acts as a non-ATP competitive inhibitor. Then we explored that whether there is a competitive relationship between **6v** and GS-2. In these experiments, GS-2 concentrations varied and ATP concentration was kept unchanged as the activities of **6v** were measured at concentrations of 25 μM and 50 μM separately. The results were showed in Fig. 3B and the double reciprocal plotting of the data in this figure indicates that compound **6v** acts as a noncompetitive inhibitor of GS-2.

To further investigate the interaction feature of BTZs to the enzyme, the inhibitory activities of compound **6v** at different preincubation time were measured and the results were shown in Fig. 3C. Normally, the inhibition effect of reversible inhibitors does not increase at different incubation time, while an irreversible inhibitor increases the inhibition percentage as it increases the time of incubation with the enzyme. As could be seen in Fig. 3C, the activities of **6v** were almost kept unchanged with the increasing of the pre-incubation time, which indicates compound **6v** acts as a reversible GSK-3β inhibitor.

2.2.3. Kinase selectivity studies

High selectivity of protein kinase inhibitors is critical to avoid widespread effects in a potential therapy. Thus for evaluating the selectivity of BTZ compounds as potential inhibitors, the representative compound **6v** was assayed against a panel of other 13 kinases. These kinases include four serine/threonine kinases as Cdk-1/cyclin B, CK-II, PKA and PKCα which are highly close to GSK-3β, and nine tyrosine kinases as Flt-1, KDR, PDGFR-β, EPH-A2, EGFR, ErbB2, ErbB4, RON and Abl, which play important role in cancer signaling pathways. All of the inhibitory assays were carried out at a 100 μM of **6v** concentration. The serine/threonine kinases inhibition were performed at Millipore Corporation (Dundee, UK) by KinaseProfiler™ service, and the tyrosine kinases screen was assayed utilizing an ELISA approach as described in Experimental section. The results listed in Table 2 showed that compound **6v** almost displayed no inhibitory activity against the whole set of kinases, which to some extent demonstrates that BTZs might have good specificity with respect to GSK-3β.

2.2.4. Structure–activity relationships (SAR) analysis

In order to explore the main features between the chemical structures and their GSK-3β inhibition, a preliminary structure–activity relationship of BTZs was analyzed based on the preceding *in vitro* data, which were listed in Table 1. The substituents R^2 attached to the *N*5 of the BTZ ring seemed to be important for keeping the activities, of which the benzyl group was the best one (**6f** vs **6a**–**e**) in the test set. Furthermore, ortho-nitro group and meta-carbomethoxy group could dramatically contribute to the inhibitory potency as attached to the benzyl moiety (**6l**, **6t**).

On the other hand, the size and nature of the substituents R^1 attached to the *C*2 should also be crucial for inhibition. The

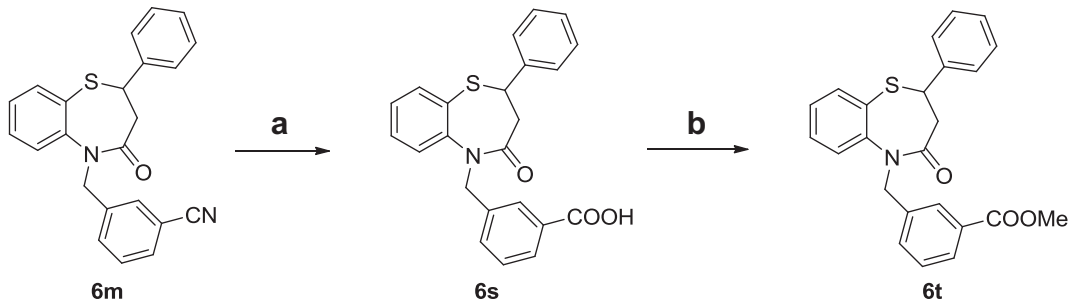

Scheme 2. Reagents and conditions: (a) conc. HCl, 100 °C, 7 h; (b) $SOCl_2$, MeOH, reflux.

Table 1
GSK-3β inhibitory activities of compounds **6a**–**6y**.

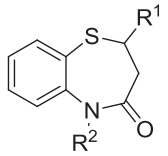

Compound	R^1	R^2	IC_{50} (μM)[a]
6a	2-Thienyl	Et	>100
6b	2-Thienyl	^{i}Pr	>100
6c	2-Thienyl	^{n}Bu	>100
6d	2-Thienyl	Cyclohexthylmethyl	>100
6e	2-Thienyl	Benzoyl	>100
6f	2-Thienyl	Bn	47.5
6g	2-Furyl	Bn	77.2
6h	H	Bn	>100
6i	Me	Bn	>100
6j	3-Pyridyl	Bn	>100
6k	Ph	Bn	42.7
6l	Ph	2-NO_2–Bn	25.0
6m	Ph	2-CN–Bn	>100
6n	Ph	2-F-Bn	>100
6o	Ph	2-Cl-Bn	>100
6p	Ph	2-Br-Bn	73.9
6q	Ph	2-CH_3–Bn	76.1
6r	Ph	4-CH_3O–Bn	73.7
6s	Ph	3-COOH–Bn	>100
6t	Ph	3-COOMe–Bn	27.8
6u	Ph	3-Cl–PhCOCH$_2$	37.8
6v	PhCH$_2$	2-NO_2–Bn	23.0
6w	4-F–Ph	2-NO_2–Bn	81.5
6x	4-Cl–Ph	2-NO_2–Bn	71.3
6y	4-Br–Ph	2-NO_2–Bn	67.8
TDZD-8[b]	–	–	1.4

[a] IC_{50}, the mean value of at least two separate determinations, each determination was mean of triplicate experiments.
[b] TDZD-8, the first reported non-ATP competitive GSK-3β inhibitor, was used as reference compound in this study.

compounds with methyl moiety or without substituent at *C*2 did not show any activities (**6h**, **6i**). However, the inhibition potency was enhanced considerably when aromatic groups, such as thienyl, furyl, phenyl and benzyl (**6f**, **6g**, **6k** and **6v**) were introduced to *C*2, suggesting favorable hydrophobic interactions with the enzyme.

In a summary, the presence of both a bulky hydrophobic substituent at *N*5 position and an aromatic group at *C*2 position in the BTZ scaffold (**6l**, **6t**, **6u** and **6v**) seems favorable to increase the GSK-3β inhibitory activity.

Table 2
Inhibitory activity (% inhibition) of compound **6v** (100 μM) against several protein kinases.

Serine/threonine kinases	% Inhibition	Tyrosine kinases	% Inhibition	Tyrosine kinases	% Inhibition
Cdk-1/cyclin B	1.5	Flt-1[a]	0.6	ErbB4[b]	0
CK-II	0	KDR[a]	5.3	EPH-A2[c]	−24.3
PKA	0	PDGFR-β[a]	−81.8	Abl[c]	18.1
PKCα	12.0	EGFR[b]	0	RON[d]	0
–	–	ErbB2[b]	2.7	–	–

[a] **Su11248** as reference inhibitor for Flt-1 (87.1% inhibition), KDR (89.7% inhibition) and PDGFR-β (82.1% inhibition).
[b] **BIBW2992** as reference inhibitor for EGFR (86.9% inhibition), ErbB2 (79.4% inhibition) and ErbB4 (82.8% inhibition).
[c] **Dasatinib** as reference inhibitor for EPH-A2 (83.1% inhibition), Abl (90.0% inhibition).
[d] **PD173074** as reference inhibitor for RON (93.4% inhibition).

2.2.5. Molecular docking

In order to gain an in-depth understanding on the interaction mechanism for BTZs within the non-ATP binding pocket of GSK-3β, a docking study of compound **6v** was performed utilizing the GOLD 5.0 [21] software. The GSK-3β crystal structure as PDB ID of 1PYX was chosen as the model of receptor because it was lately proven to be the best one for the non-ATP binding in a docking study with three GSK-3β crystal structures (PDB ID: 1PYX, 1Q41, and 1Q4L) [22]. The ligand was prepared by minimizing the energy of compound **6v** using Sybyl 6.9 [31] with the MMFF94 force, and the binding site was defined as a sphere of 10 Å radius around the residue Arg 209, which is suggested to be a key residue for GSK-3β binding process [22]. The suggested binding mode was shown in Fig. 4 and several key interactions were observed. Compound **6v** was located between residues Arg 209 and Ser 236, and its BTZ ring bound with Arg 209 by cation-π interaction. In addition, there were two hydrogen bonds formed between **6v** and the binding pocket. One hydrogen bond was attributed to the oxygen of carbonyl on BTZ ring with Arg 209, and the other one interacted between nitro group of the compound and Ser 236. Finally, *C*2-subsitituted group of the inhibitor was extended to the hydrophobic region consisting of three amino residues (Leu 169, Pro 331 and Thr 330). This docking mode can well explain the inhibitory activity of compound **6v** to GSK-3β. It is worth to note that this result is also consistent with the recently proposed hypothesis by Martinez et al. [22], which assumed that three key residues (Arg 209, Thr 235, Ser 236)

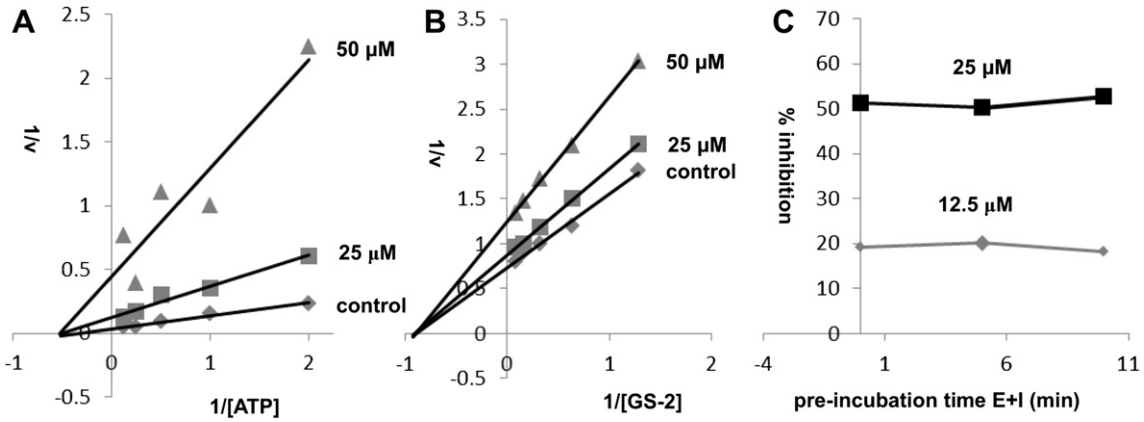

Fig. 3. Kinetic data determined for the compound **6v**. (A) ATP concentrations varied from 0.5 μM to 8 μM in the reaction mixture; GS-2 concentration was kept constant at 6.25 μM; compound concentrations were depicted in the plot. (B) GS-2 concentrations varied from 0.78 μM to 12.5 μM in the reaction mixture; ATP concentration was kept constant at 2 μM; compound concentrations were depicted in the plot. (C) Time dependent GSK-3β inhibition of **6v**. Each point was the mean of two separate experiments and each experiment performed in triplicate.

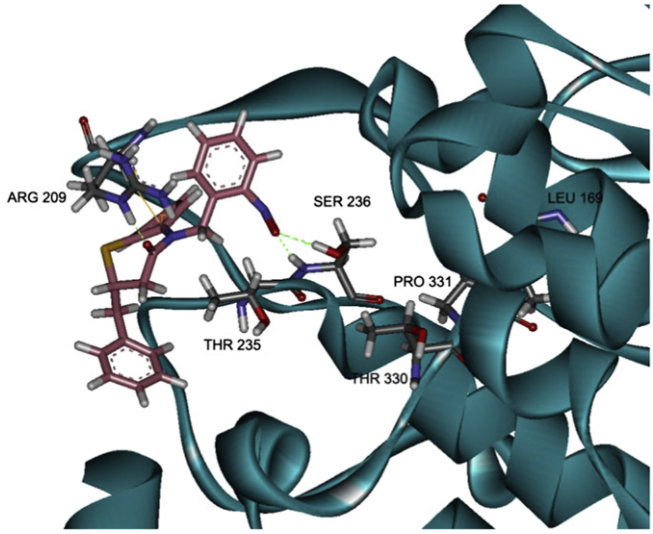

Fig. 4. Suggested binding mode for compound **6v** in GSK-3β (PDB ID: 1PYX).

in an allosteric binding site are potentially related to the active conformation of GSK-3β. Therefore, it is hoped that the present work will be helpful for further study of more potent GSK-3β inhibitors.

2.2.6. Predicting ADME properties

Finally, the ADME descriptors module available in Discovery Studio (DS) 3.0 [23] was used to predict a range of drug-like properties for the compound **6v**. This protocol uses the QSAR models and is suitable to estimate the ADME related properties for small molecules. The following properties, and classes of properties, can be computed such as human intestinal absorption (HIA), aqueous solubility, blood–brain barrier penetration (BBB), cytochrome P450 (CYP450) 2D6 inhibition and plasma protein binding. The resulted data were listed in Table 3. It showed compound **6v** might have good intestinal absorption after oral administration and medium ability to cross the blood–brain barrier (BBB), but its aqueous solubility predicted was not so good. In addition, compound **6v** was likely to inhibit CYP2D6 enzyme, which belongs to CYP450 enzyme family. The results also showed that the binding between inhibitor and plasma protein is less than 90%, which means the compound is unlikely to be highly bound to carrier proteins in the blood. However, it is a common experience that ADME properties are difficult to predict accurately just by *in silico* and so the predicted properties should be used with caution. For our study, more experiments should be done to explore the real properties of these compounds.

Table 3
ADME properties of compound **6v** predicted.

	Value	Level
Absorption[a]	NV[b]	0
Solubility[c]	−4.619	2
BBB[d]	−0.06	2
CYP2D6[e]	0.722	1
PPB[f]	NV	0
AlogP98[f]	3.733	0

[a] Level 0 means inhibitor has good human intestinal absorption (HIA) after oral administration.
[b] NV means no value was given.
[c] Level 2 means the aqueous solubility of inhibitor is not very good and its drug-likeness properties are low.
[d] Level 2 means inhibitor has medium ability to cross the blood–brain barrier (BBB).
[e] Level 1 means inhibitor likely to inhibit CYP2D6 enzyme.
[f] Level 0 means the binding between inhibitor and plasma protein is less than 90% (No markers flagged and AlogP98 < 4.0).

3. Conclusion

In summary, we have disclosed a novel series of BTZ compounds as non-ATP competitive GSK-3β inhibitors. Based on the structure modification of the hits found from a structure-based docking screening, twenty five BTZ derivatives were successfully synthesized and the *in vitro* luminescent bioassay showed that about half of them can inhibit GSK-3β with IC_{50} values in micromolar level. Among them, three compounds **6l**, **6t** and **6v** have IC_{50} values of 25.0 μM, 27.8 μM and 23.0 μM respectively. As the representative, compound **6v** is proved to reversibly inhibit GSK-3β as non-ATP competitive mechanism through kinetic analysis. Moreover, it almost has not shown any inhibitory activity to a whole panel of other 13 protein kinases, which to some extent suggests good specificity of BTZ compounds with respect to GSK-3β. The results of our primary SAR study also remind us that the nature of BTZ moiety and certain substituents would be important for retaining GSK-3β inhibition. The presence of both a bulky hydrophobic substituent at *N*5 position and an aromatic group at *C*2 position in BTZ scaffold seem crucial to increase the inhibitory activity. Finally, the binding mode of compound **6v** to a non-ATP binding pocket of GSK-3β was established by molecular docking and several key interactions were observed. In this binding mode, the affinity seems mainly attributed to the hydrogen-bonds interaction by the carbonyl and nitro groups of inhibitor **6v** with Arg 209 and Ser 236 respectively, which let the compound more closely bind to the pocket of enzyme and contributed to the inhibitory activity. According to our work, it is hoped that the inhibitory potency and specificity of BTZs toward GSK-3β should allow them worth to further study as potential therapeutic candidates for severe unmet human diseases where GSK-3β is up-regulated.

4. Experimental

4.1. Chemistry

Reagents were purchased from commercial sources and then used without further purification except special case. Flash column chromatography was carried out at medium pressure using silica gel (200–300 mesh) purchased from Qingdao Haiyang Chemical Co. Ltd. All the reactions were monitored by thin layer chromatography (TLC) on silica gel. ^{1}H NMR and ^{13}C NMR spectra were obtained on Mercury Plus 400 spectrometers working at 400 MHz and 100 MHz, respectively. Chemical shifts (δ) are reported in parts per million (ppm) relative to internal tetramethylsilane (TMS) and *J* values are reported in Hertz. MS spectra were recorded on an Agilent LC-MS 1100 instrument with an ESI mass selective detector. Melting points were determined by an SGW X-4 thermometer and were uncorrected (slide method).

4.1.1. General procedure for the synthesis of 3-substituted acrylic acid

A mixture of substituted carbaldehyde (200 mmol), propenedioic acid (20.8 g, 200 mmol) in a solution of pyridine (10 ml, 120 mmol) and piperidine (1 ml) was warmed at reflux for 2 h. The resultant solution was poured into 2 M HCl aq. and then cooled to room temperature. The present solid was collected by filtration, washed with water and recrystallized from ethanol/water.

*4.1.1.1. 3-(2-thienyl)acrylic acid (**4a**).* Yield: 85%; mp 158.2–159.6 °C (lit. mp 153–154 °C [24]).

*4.1.1.2. 3-(2-Furyl)acrylic acid (**4b**).* Yield: 69%; mp 138.3–142.7 °C (lit. mp 141–143 °C [25]).

*4.1.1.3. 3-(3-Pyridyl)acrylic acid (**4e**).* Yield: 92%; mp 231.6–234.5 °C (lit. mp 233 °C [26]).

*4.1.1.4. 3-Phenylacrylic acid (**4f**).* Yield: 91%; mp 134.6–135.7 °C (lit. mp 132–133 °C [26]).

*4.1.1.5. 3-Benzylacrylic acid (**4g**).* Yield: 56%; mp 63.2–64.6 °C (lit. mp 64–65 °C [27]).

*4.1.1.6. 3-(4-Fluorophenyl)acrylic acid (**4h**).* Yield: 88%; mp 205.8–207.4 °C (lit. mp 209–210 °C [28]).

*4.1.1.7. 3-(4-Chlorophenyl)acrylic acid (**4i**).* Yield: 95%; mp 247.1–250.5 °C (lit. mp 248 °C [29]).

*4.1.1.8. 3-(4-Bromophenyl)acrylic acid (**4j**).* Yield: 85%; mp 255.9–257.6 °C (lit. mp 253 °C [29]).

4.1.2. General procedure for the synthesis of 2,3-dihydro-2-substituted-1,5-benzothiazepin-4(5H)-one

A mixture of 3-substituted-acrylic acid (106 mmol), 2-aminobenzenetiol (13.3 g, 106 mmol) and 4 Å molecular sieve was heated at 180 °C under nitrogen atmosphere for 6 h, then acetonitrile (80 ml) was added and the solution was cooled to room temperature. The resultant solid was collected by filtration and washed with acetonitrile.

*4.1.2.1. 2,3-Dihydro-2-(2-thienyl)-1,5-benzothiazepin-4(5H)-one (**5a**).* Yield: 66%; mp 172.6–173.4 °C; ^{1}H NMR (400 MHz, $CDCl_3$) δ 7.67–7.14 (m, 5H), 6.96–6.91 (m, 2H), 5.16 (dd, J = 5.8 Hz, 11.0 Hz, 1H), 2.97–2.81 (m, 2H). ESI-MS (positive): 262.0 $(M + 1)^+$.

*4.1.2.2. 2,3-Dihydro-2-(2-furyl)-1,5-benzothiazepin-4(5H)-one (**5b**).* Yield: 60%; mp 162.7–163.6 °C; ^{1}H NMR (400 MHz, $CDCl_3$) δ 8.19 (bs, 1H), 7.59–7.15 (m, 5H), 6.30 (d, J = 1.2 Hz, 1H), 6.16 (d, J = 3.1 Hz, 1H), 4.93 (dd, J = 6.3 Hz, 11.0 Hz, 1H), 2.93–2.82 (m, 2H). ESI-MS (positive): 246.1 $(M + 1)^+$.

*4.1.2.3. 2,3-Dihydro-1,5-benzothiazepin-4(5H)-one (**5c**).* Yield: 31%; mp 214.3–216.8 °C; ^{1}H NMR (400 MHz, $CDCl_3$) δ 7.83 (s, 1H), 7.62–7.58 (d, J = 1.4 Hz, 1H), 7.38–7.34 (m, 1H), 7.19–7.15 (m, 1H), 7.11–7.08 (d, J = 7.9 Hz, 1H), 3.47–3.43 (m, 2H), 2.65–2.61 (m, 2H). ESI-MS (positive): 180.1 $(M + 1)^+$.

*4.1.2.4. 2,3-Dihydro-2-methyl-1,5-benzothiazepin-4(5H)-one (**5d**).* Yield: 51%; mp 209.1–212.5 °C; ^{1}H NMR (400 MHz, $CDCl_3$) δ 7.83 (s, 1H), 7.65–7.52 (m, 1H), 7.42–7.30 (m, 1H), 7.21–7.15 (m, 1H), 7.14–7.04 (m, 1H), 3.92–3.81 (m, 1H), 2.72–2.58 (m, 1H), 2.40–2.26 (m, 1H), 1.48–1.39 (d, J = 6.6 Hz, 3H). ESI-MS (positive): 194.1 $(M + 1)^+$.

*4.1.2.5. 2,3-Dihydro-2-(3-pyridyl)-1,5-benzothiazepin-4(5H)-one (**5e**).* Yield: 25%; mp 188.2–190.3 °C; ^{1}H NMR (400 MHz, $CDCl_3$) δ 8.71 (bs, 1H), 8.51 (dd, J = 1.5 Hz, 5.0 Hz, 1H), 8.46 (d, J = 1.5 Hz, 1H), 7.56 (d, J = 7.5 Hz, 1H), 7.32 (d, J = 8.0 Hz, 1H), 7.25–7.19 (m, 2H), 7.05 (td, J = 1.5, 8.0 Hz, 1H), 6.88 (dd, J = 1.0 Hz, 8.0 Hz, 1H), 3.64 (dd, J = 5.5 Hz, 9.5 Hz, 1H), 3.31 (dd, J = 5.0 Hz, 14.0 Hz, 1H), 2.87 (dd, J = 9.5 Hz, 14.0 Hz, 1H). ESI-MS (positive): 257.1 $(M + 1)^+$.

*4.1.2.6. 2,3-Dihydro-2-phenyl-1,5-benzothiazepin-4(5H)-one (**5f**).* Yield: 25%; mp 177.6–179.9 °C; ^{1}H NMR (400 MHz, $CDCl_3$) δ 8.30 (bd, 1H), 7.42–7.17 (m, 9H), 4.87–4.91 (m, 1H); 2.94–2.79 (m, 2H); ESI-MS (positive): 256.1 $(M + 1)^+$.

*4.1.2.7. 2,3-Dihydro-2-benzyl-1,5-benzothiazepin-4(5H)-one (**5g**).* Yield: 24%; mp 138.2–141.3 °C; ^{1}H NMR (400 MHz, $CDCl_3$) δ 8.25–5.99 (m, 9H), 4.12–3.85 (m, 1H), 3.72 (q, J = 7.0 Hz, 1H), 3.14–2.76 (m, 2H), 2.58 (dd, J = 12.4, 5.7 Hz, 1H), 2.39 (dd, J = 12.5, 8.8 Hz, 1H); ^{13}C NMR (100 MHz, $CDCl_3$) δ 172.3, 141.4, 137.9, 136.1, 130.0, 129.4, 128.5, 126.8, 126.6, 126.4, 123.0, 51.0, 43.4, 38.6; ESI-MS (positive): 270.1 $(M + 1)^+$.

*4.1.2.8. 2,3-Dihydro-2-(4-fluorophenyl)-1,5-benzothiazepin-4(5H)-one (**5h**).* Yield: 30%; mp 182.9–184.0 °C; ^{1}H NMR (400 MHz, $CDCl_3$) δ 8.88 (s, 1H), 7.93–6.54 (m, 8H), 4.89 (dd, J = 10.4, 6.1 Hz, 1H), 3.15–2.53 (m, 2H); ESI-MS (positive): 274.1 $(M + 1)^+$.

*4.1.2.9. 2,3-Dihydro-2-(4-chlorophenyl)-1,5-benzothiazepin-4(5H)-one (**5i**).* Yield: 28%; mp 205.4–207.9 °C; ^{1}H NMR (400 MHz, $CDCl_3$) δ 8.55 (br, 1H), 7.87–6.80 (m, 8H), 5.06–4.65 (m, 1H), 3.10–2.52 (m, 2H); ESI-MS (positive): 289.9 $(M + 1)^+$.

*4.1.2.10. 2,3-Dihydro-2-(4-bromophenyl)-1,5-benzothiazepin-4(5H)-one (**5j**).* Yield: 32%; mp 169.2–170.8 °C; ^{1}H NMR (400 MHz, DMSO-d_6) δ 8.46 (br, 1H), 7.85–6.83 (m, 8H), 5.01 (dd, J = 10.7, 5.6 Hz, 1H), 2.63 (ddd, J = 39.2, 27.9, 19.5 Hz, 2H). ESI-MS (positive): 334.0, 336.0 $(M + 1)^+$.

4.1.3. General procedure for the synthesis of 2,3-dihydro-2,5-disubstituted-1,5-benzothiazepin-4(5H)-one

A mixture of 2,3-dihydro-2-substituted-1,5-benzothiazepin-4(5*H*)-one (2 mmol) and 80% NaH (0.18 g, 6 mmol) in anhydrous DMF (8 ml) were stirred at −10 °C for 0.5 h. Then alkyl/acyl chloride (1.2 mmol) was added and the mixture was kept under stirring at −10 °C for 1–20 h. The reaction was quenched by saturated aqueous NH_4Cl and the product was extracted by ethyl acetate, washed with water and brine, dried over Na_2SO_4 and then subjected to flash chromatograph.

*4.1.3.1. 2,3-Dihydro-2-(2-thienyl)-5-ethyl-1,5-benzothiazepin-4(5H)-one (**6a**).* Yield: 65%; mp 104.6–105.6 °C; ^{1}H NMR (400 MHz, $CDCl_3$) δ 7.96–6.53 (m, 7H), 5.10 (dd, J = 12.5, 5.4 Hz, 1H), 4.33 (dq, J = 14.2, 7.2 Hz, 1H), 3.56 (dq, J = 14.0, 7.0 Hz, 1H), 3.07–2.44 (m, 2H), 1.20 (dt, J = 14.2, 10.5 Hz, 3H). ^{13}C NMR (100 MHz, $CDCl_3$) δ 169.9, 147.8, 146.1, 136.9, 130.6, 127.1, 126.7, 124.5, 124.3, 123.5, 48.5, 43.9, 42.9, 12.9; ESI-MS (positive): 290.0 $(M + 1)^+$.

*4.1.3.2. 2,3-Dihydro-2-(2-thienyl)-5-isopropyl-1,5-benzothiazepin-4(5H)-one (**6b**).* Yield: 50%; mp 76.1–78.8 °C; ^{1}H NMR (400 MHz, $CDCl_3$) δ 7.64–7.14 (m, 5H), 6.88 (dd, J = 3.5, 5.1 Hz, 1H), 6.79 (d, J = 3.1 Hz, 1H), 5.06 (dd, J = 5.5 Hz, 12.5 Hz, 1H), 4.90 (m, 1H), 2.86 (m, 1H), 2.63–2.57 (m, 1H), 1.45 (d, J = 6.7 Hz, 3H), 1.05 (d, J = 6.7 Hz, 3H); ^{13}C NMR (100 MHz, $CDCl_3$) δ 169.8, 147.7, 144.6, 137.1, 130.1, 128.1, 127.7, 127.5, 126.7, 126.5, 126.0, 124.5, 123.5, 49.3, 48.1, 43.3, 22.7, 20.0; ESI-MS (positive): 304.1 $(M + 1)^+$.

*4.1.3.3. 2,3-Dihydro-2-(2-thienyl)-5-n-butyl-1,5-benzothiazepin-4(5H)-one (**6c**).* Yield: 62%; mp 83.9–84.6 °C; ^{1}H NMR (400 MHz, $CDCl_3$) δ 7.91–6.47 (m, 7H), 5.13 (dd, J = 12.6, 5.4 Hz, 1H), 4.24 (dd, J = 13.6, 8.4 Hz, 1H), 3.31 (dd, J = 13.6, 6.0 Hz, 1H), 3.04–2.52 (m, 2H), 2.13–1.58 (m, 1H), 1.22 (s, 1H), 1.00 (dd, J = 10.9, 6.7 Hz, 2H), 0.84 (t, J = 8.0 Hz, 3H). ^{13}C NMR (100 MHz, $CDCl_3$) δ 170.0, 147.9, 146.4, 137.2, 130.5, 126.8, 126.7, 124.5, 123.9, 123.5, 55.3, 50.9, 48.5, 43.1, 27.7, 20.7, 20.7; ESI-MS (positive): 318.1 $(M + 1)^+$.

*4.1.3.4. 2,3-Dihydro-2-(2-thienyl)-5-cyclohexthylmethyl-1,5-benzothiazepin-4(5H)-one (**6d**).* Yield: 15%; mp 142.5–143.2 °C; ^{1}H NMR (400 MHz, $CDCl_3$) δ 7.84–6.52 (m, 7H), 5.23 (d, J = 15.0 Hz, 1H), 5.08–4.70 (m, 2H), 3.10–2.60 (m, 2H), 1.98–1.08 (m, 11H). ^{13}C NMR (100 MHz, $CDCl_3$) δ 170.6, 158.8, 146.1, 143.9, 136.5, 130.1, 129.4, 129.1, 128.7, 127.6, 127.5, 127.1, 126.1, 124.2, 55.2, 52.9, 51.1, 50.8, 42.1, 29.7; ESI-MS (positive): 358.1 $(M + 1)^+$.

*4.1.3.5. 2,3-Dihydro-2-(2-thienyl)-5-benzoyl-1,5-benzothiazepin-4(5H)-one (**6e**).* Yield: 89%; mp 234.8–235.6 °C; ^{1}H NMR (400 MHz, $CDCl_3$) δ 8.26–6.58 (m, 12H), 5.12 (dd, J = 11.1, 6.1 Hz, 1H), 3.01 (ddd, J = 23.5, 12.3, 8.7 Hz, 2H); ^{13}C NMR (100 MHz, $CDCl_3$) δ 172.3, 170.3, 143.2, 137.6, 134.3, 133.1, 130.9, 129.6, 128.6, 128.5, 126.9, 126.6, 125.0, 124.2, 47.4, 43.5; ESI-MS (positive): 366.1 $(M + 1)^+$.

*4.1.3.6. 2,3-Dihydro-2-(2-thienyl)-5-benzyl-1,5-benzothiazepin-4(5H)-one (**6f**).* Yield: 86%; mp 143.7–145.1 °C; ^{1}H NMR (400 MHz, $CDCl_3$) δ 7.58–7.15 (m, 10H), 6.90–6.88 (m, 1H), 5.99 (d, J = 3.5 Hz, 1H), 5.19 (d, J = 14.9 Hz, 1H), 5.14 (m, 1H), 5.01 (d, J = 14.9 Hz, 1H), 3.00 (m, 1H), 2.85–2.79 (m, 1H); ^{13}C NMR (100 MHz, $CDCl_3$) δ 170.1, 147.7, 146.1, 137.1, 137.0, 133.4, 130.8, 130.5, 129.3, 128.4, 128.0, 127.3, 127.1, 126.7, 126.5, 124.6, 123.9, 123.6, 58.5, 51.8, 48.5, 42.9; ESI-MS (positive): 352.1 $(M + 1)^+$.

*4.1.3.7. 2,3-Dihydro-2-(2-furyl)-5-benzyl-1,5-benzothiazepin-4(5H)-one (**6g**).* Yield: 75%; mp 104.9–105.7 °C; ^{1}H NMR (400 MHz, $CDCl_3$) δ 7.47–7.14 (m, 10H), 6.26 (s, 1H), 5.99 (d, J = 2.4 Hz, 1H), 5.17 (d, J = 15.3 Hz, 1H), 5.01 (d, J = 15.3 Hz, 1H), 4.89 (dd, J = 5.9, 12.6 Hz, 1H), 2.92–2.81 (m, 2H); ^{13}C NMR (100 MHz, $CDCl_3$) δ 170.4, 154.9, 146.1, 142.2, 137.0, 136.0, 130.3, 128.4, 128.0, 127.3, 127.0, 126.7, 123.8, 110.3, 105.3, 58.5, 51.8, 45.9, 38.8; ESI-MS (positive): 336.1 $(M + 1)^+$.

*4.1.3.8. 2,3-Dihydro-5-benzyl-1,5-benzothiazepin-4(5H)-one (**6h**).* Yield: 78.7%; mp 104.7–105.8 °C; ^{1}H NMR (400 MHz, $CDCl_3$) δ 7.57–7.55 (d, J = 1.6 Hz, 1H), 7.35–7.19 (m, 7H), 7.16–7.13 (m, 1H), 5.18–4.98 (m, 2H), 3.5–3.3 (m, 2H), 2.7–2.5 (m, 2H); ^{13}C NMR (100 MHz, $CDCl_3$) δ 172.0, 146.4, 137.2, 135.9, 129.9, 128.3, 128.2, 127.9, 127.2, 124.1, 51.8, 34.5, 34.2; ESI-MS (positive): 270.1 $(M + 1)^+$.

*4.1.3.9. 2,3-Dihydro-2-methyl-5-benzyl-1,5-benzothiazepin-4(5H)-one (**6i**).* Yield: 79.5%; mp 115.6–117.9 °C; ^{1}H NMR (400 MHz, $CDCl_3$) δ 7.6–7.48 (d, J = 7.4 Hz, 1H), 7.41–7.18 (m, 7H), 7.18–7.07 (m, 1H), 5.16–5.06 (d, J = 15.3 Hz, 1H), 5.06–4.88 (d, J = 15.3 Hz, 1H), 3.90–3.55 (m, 1H), 2.70–2.55 (m, 1H), 2.36–2.17 (m, 1H), 1.32–1.26 (d, J = 6.6 Hz, 3H); ^{13}C NMR (100 MHz, $CDCl_3$) δ 171.4, 146.3, 137.2, 136.8, 135.4, 130.4, 129.8, 128.3, 128.0, 127.6, 127.2, 126.8, 123.8, 51.7, 45.1, 42.5, 24.3; ESI-MS (positive): 284.2 $(M + 1)^+$.

*4.1.3.10. 2,3-Dihydro-2-(3-pyridyl)-5-benzyl-1,5-benzothiazepin-4(5H)-one (**6j**).* Yield: 60%; mp 178.9–180.2 °C; ^{1}H NMR (400 MHz, $CDCl_3$) δ 8.52 (d, J = 4.7 Hz, 1H), 8.43 (s, 1H), 7.57 (dd, J = 2.0 Hz, 7.8 Hz, 1H), 7.35–7.00 (m, 10H), 5.32 (d, J = 16.0 Hz, 1H), 5.16 (d, J = 16.0 Hz, 1H), 3.71 (dd, J = 5.1, 9.8 Hz, 1H), 3.36 (dd, J = 5.1, 14.1 Hz, 1H), 2.86 (dd, J = 9.8, 14.5 Hz, 1H); ^{13}C NMR (100 MHz, $CDCl_3$) δ 166.5, 150.4, 148.2, 139.2, 137.1, 136.6, 132.9, 129.1, 128.8, 127.5, 127.3, 126.2, 124.0, 123.4, 121.2, 117.9, 48.9, 44.8, 32.0; ESI-MS (positive): 347.2 $(M + 1)^+$.

*4.1.3.11. 2,3-Dihydro-2-phenyl-5-benzyl-1,5-benzothiazepin-4(5H)-one (**6k**).* Yield: 89%; mp 146.7–150.6 °C; ^{1}H NMR (400 MHz, $CDCl_3$) δ 7.58–7.14 (m, 14H), 5.23 (d, J = 15.2 Hz), 1H, 5.01 (d, J = 15.2 Hz, 1H), 4.88–4.83 (m, 1H), 2.94–2.82 (m, 2H); ^{13}C NMR (100 MHz, $CDCl_3$) δ 170.7, 146.2, 144.0, 137.1, 136.6, 130.2, 128.8, 128.4, 128.0, 127.7, 127.3, 127.2, 126.1, 124.1, 52.9, 51.8, 42.1; ESI-MS (positive): 346.1 $(M + 1)^+$.

*4.1.3.12. 2,3-Dihydro-2-phenyl-5-(2-nitrobenzyl)-1,5-benzothiazepin-4(5H)-one (**6l**).* Yield: 75%; mp 186.7–189.5 °C; ^{1}H NMR (400 MHz, $CDCl_3$) δ 8.24–6.88 (m, 13H), 5.54 (d, J = 25.7 Hz, 2H), 5.06–4.73 (m, 1H), 3.15–2.74 (m, 2H); ^{13}C NMR (100 MHz, $CDCl_3$) δ 171.0, 148.1, 145.8, 143.6, 136.8, 133.7, 132.7, 130.7, 129.6, 128.8, 128.0, 127.8, 127.4, 127.1, 126.1, 125.0, 123.4, 52.9, 50.9, 49.5, 42.1, 29.7; ESI-MS (positive): 390.9 $(M + 1)^+$.

*4.1.3.13. 2,3-Dihydro-2-phenyl-5-(2-cyanobenzyl)-1,5-benzothiazepin-4(5H)-one (**6m**).* Yield: 88%; mp 148.6–149.8; ^{1}H NMR (400 MHz, $CDCl_3$) δ 8.02–6.96 (m, 13H), 5.69 (d, J = 16.0 Hz, 1H), 5.12 (d, J = 16.0 Hz, 1H), 4.87 (dd, J = 12.6, 5.6 Hz, 1H), 2.90 (dd, J = 15.9, 9.1 Hz, 2H); ^{13}C NMR (100 MHz, $CDCl_3$) δ 170.7, 145.4, 143.6, 138.3, 136.8, 132.6, 131.6, 131.1, 130.5, 129.2, 128.8, 127.8, 127.6, 126.0, 123.9, 118.7, 112.4, 52.8, 51.1, 41.8, 31.9, 29.7; ESI-MS (positive): 370.8 $(M + 1)^+$.

*4.1.3.14. 2,3-Dihydro-2-phenyl-5-(2-flurobenzyl)-1,5-benzothiazepin-4(5H)-one (**6n**).* Yield: 87%; mp 143.2–146.4 °C; ^{1}H NMR (400 MHz, $CDCl_3$) δ 7.96–6.57 (m, 13H), 5.50–4.95 (m, 2H), 4.85 (dd, J = 12.6, 5.5 Hz, 1H), 3.12–2.62 (m, 2H); ^{13}C NMR (100 MHz, $CDCl_3$) δ 170.8, 145.9, 143.9, 136.5, 130.3, 130.31, 130.27, 129.00, 128.92, 128.76, 127.69, 127.30, 127.24, 126.08, 124.13, 124.09, 123.95, 123.91, 123.76, 115.13, 114.91, 52.82, 44.90, 44.86, 42.01. ESI-MS (positive): 364.1 $(M + 1)^+$.

*4.1.3.15. 2,3-Dihydro-2-phenyl-5-(2-chlorobenzyl)-1,5-benzothiazepin-4(5H)-one (**6o**).* Yield: 100%; mp 169.3–172.5 °C; ^{1}H NMR (400 MHz, $CDCl_3$) δ 7.99–6.66 (m, 13H), 5.26 (s, 2H), 4.89 (dd, J = 12.8, 5.2 Hz, 1H), 3.18–2.74 (m, 2H); ^{13}C NMR (100 MHz, $CDCl_3$) δ 170.9, 146.0, 143.8, 136.6, 134.3, 132.8, 130.4, 129.3, 129.0, 128.8, 128.4, 127.8, 127.3, 127.1, 126.1, 124.5, 123.6, 52.9, 50.9, 49.3, 42.1, 29.7; ESI-MS (positive): 380.0 $(M + 1)^+$.

*4.1.3.16. 2,3-Dihydro-2-phenyl-5-(2-bromobenzyl)-1,5-benzothiazepin-4(5H)-one (**6p**).* Yield: 71%; mp 168.6–170.4 °C; ^{1}H NMR (400 MHz, $CDCl_3$) δ 7.91–6.66 (m, 13H), 5.24 (d, J = 4.6 Hz, 2H), 4.91 (s, 1H), 2.93 (dd, J = 26.2, 8.9 Hz, 2H); ^{13}C NMR (100 MHz, $CDCl_3$) δ 170.8, 146.1, 143.8, 136.6, 135.9, 132.6, 130.4, 129.0, 128.8, 128.7, 127.8, 127.6, 127.2, 127.1, 126.1, 123.6, 122.8, 52.9, 51.9, 42.1, 31.4, 29.7; ESI-MS (positive): 424.0, 426.4 $(M + 1)^+$.

*4.1.3.17. 2,3-Dihydro-2-phenyl-5-(2-methylbenzyl)-1,5-benzothiazepin-4(5H)-one (**6q**).* Yield: 85%; mp 133.2–134.6 °C; ^{1}H NMR (400 MHz, $CDCl_3$) δ 7.85–6.71 (m, 13H), 5.10 (dd, J = 63.2, 15.9 Hz, 2H), 4.87 (dd, J = 12.7, 5.1 Hz, 1H), 3.10–2.74 (m, 2H), 2.33 (s, 3H); ^{13}C NMR (100 MHz, $CDCl_3$) δ 170.6, 146.4, 144.0, 136.5, 135.7, 134.8, 130.3, 130.1, 128.8, 127.7, 127.3, 127.2, 127.1, 126.1, 126.0, 123.9, 58.5, 52.9, 49.7, 42.2, 19.3, 18.4; ESI-MS (positive): 360.1 $(M + 1)^+$.

*4.1.3.18. 2,3-Dihydro-2-phenyl-5-(4-methoxylbenzyl)-1,5-benzothiazepin-4(5H)-one (**6r**).* Yield: 60%; mp 110.8–113.1 °C; ^{1}H NMR (400 MHz, $CDCl_3$) δ 8.07–6.50 (m, 7H), 5.12 (dd, J = 12.6, 5.4 Hz, 1H), 4.23 (dd, J = 13.7, 7.8 Hz, 1H), 3.75 (s, 3H), 3.31 (dd, J = 13.7, 5.8 Hz, 1H), 3.07–2.46 (m, 2H); ^{13}C NMR (100 MHz, $CDCl_3$) δ 170.0, 147.9, 146.6, 137.2, 130.5, 127.0, 126.7, 126.6, 126.5, 124.5, 123.9, 123.5, 54.6, 50.9, 48.9, 48.5, 43.1, 37.0, 31.2; ESI-MS (positive): 376.1 $(M + 1)^+$.

*4.1.3.19. 2,3-Dihydro-2-phenyl-5-(3-carboxylbenzyl)-1,5-benzothiazepin-4(5H)-one (**6s**).* A solution of **6m** (0.2 g, 0.54 mmol) in conc. HCl (5 ml) was reflux in a sealed tube at 100 °C for 7 h, and then cooled to room temperature. The pale-yellow precipitate was collected by filtration and washed with methanol, yield: 70%, mp 186.4–188.7 °C; ^{1}H NMR (400 MHz, DMSO-d_6) δ 12.89 (s, 1H), 7.88 (s, 1H), 7.74 (d, J = 7.6 Hz, 1H), 7.62–7.16 (m, 11H), 5.44 (d, J = 15.6 Hz, 1H), 4.94 (d, J = 15.6 Hz, 1H), 4.98

(m, 1H), 2.86–2.67 (m, 2H). ^{13}C NMR (100 MHz, DMSO-d_6) δ 170.3, 167.6, 145.7, 144.3, 138.2, 136.6, 132.6, 131.2, 129.1, 129.1, 128.9, 128.5, 128.0, 127.6, 126.7, 126.5, 124.8, 52.3, 50.3, 41.7; ESI-MS (positive): 390.1 $(M + 1)^+$.

*4.1.3.20. 2,3-Dihydro-2-phenyl-5-(3-carbomethoxybenzyl)-1,5-benzothiazepin-4(5H)-one (**6t**).* To a solution of **6s** (0.04 g, 0.1 mmol) in methanol (2 ml) was added $SOCl_2$ (0.1 ml) dropwise at 0 °C under N_2 and the reaction mixture was stirred under reflux for 2 h. Then the mixture was cooled to room temperature. After the organic solvent was evaporated, the residue was purified by chromatography (petroleum ether/ethyl acetate/methanol 15:5.5:0.6) to give pale-yellow solid, Yield: 89%; mp 110.9–112.2 °C; ^{1}H NMR (400 MHz, $CDCl_3$) δ 7.98 (s, 1H), 7.92 (d, J = 7.6 Hz, 1H), 7.60 (d, J = 6.4 Hz, 2H), 7.46–7.16 (m, 9H), 5.41 (d, J = 15.2 Hz, 1H), 5.00 (d, J = 15.2 Hz, 1H), 4.89 (dd, J = 5.6 Hz, 12.4 Hz, 1H), 3.91 (s, 3H), 2.98–2.86 (m, 2H); ^{13}C NMR (100 MHz, $CDCl_3$) δ 170.8, 167.0, 145.8, 143.9, 137.4, 136.7, 132.6, 130.3, 130.2, 129.0, 128.8, 128.6, 128.6, 127.7, 127.5, 127.3, 126.1, 124.0, 52.9, 52.1, 51.4, 42.0; ESI-MS (positive): 404.2 $(M + 1)^+$.

*4.1.3.21. 2,3-Dihydro-2-phenyl-5-(2-(3-chlorophenyl)-2-oxoethyl)-1,5-benzothiazepin-4(5H)-one (**6u**).* Yield: 65%; mp 60.2–63.9 °C; ^{1}H NMR (400 MHz, $CDCl_3$) δ 8.01 (t, J = 1.6 Hz, 1H), 7.91 (d, J = 7.8 Hz, 1H), 7.65–7.16 (m, 11H), 5.76 (d, J = 17.6 Hz, 1H), 4.61 (d, J = 17.6 Hz, 1H), 4.82 (dd, J = 5.1 Hz, 12.9 Hz, 1H), 3.05–2.83 (m, 2H); ^{13}C NMR (100 MHz, $CDCl_3$) δ 192.8, 170.5, 146.7, 143.8, 136.5, 136.3, 135.2, 133.8, 130.6, 130.2, 128.8, 128.4, 127.8, 127.5, 127.0, 126.3, 126.1, 123.7, 55.9, 52.8, 41.6; ESI-MS (positive): 408.1 $(M + 1)^+$.

*4.1.3.22. 2,3-Dihydro-2-benzyl-5-(2-nitrobenzyl)-1,5-benzothiazepin-4(5H)-one (**6v**).* Yield: 95%; mp 135.0–136.9 °C; ^{1}H NMR (400 MHz, $CDCl_3$) δ 8.37–6.55 (m, 12H), 5.86–4.86 (m, 2H), 4.26–3.62 (m, 1H), 2.69 (dddd, J = 111.3, 95.2, 19.1, 9.8 Hz, 4H); ^{13}C NMR (100 MHz, $CDCl_3$) δ 171.7, 148.0, 146.1, 138.2, 137.8, 137.1, 135.9, 133.6, 133.0, 132.8, 130.5, 129.6, 129.3, 128.5, 127.9, 127.1, 126.8, 126.4, 124.9, 123.2, 51.2, 49.4, 44.1, 40.3, 37.3; ESI-MS (positive): 405.2 $(M + 1)^+$.

*4.1.3.23. 2,3-Dihydro-2-(4-fluorophenyl)-5-(2-nitrobenzyl)-1,5-benzothiazepin-4(5H)-one (**6w**).* Yield: 91%; mp 166.5–168.8 °C; ^{1}H NMR (400 MHz, $CDCl_3$) δ 8.37–6.55 (m, 12H), 5.53 (q, J = 17.3 Hz, 2H), 4.88 (dd, J = 12.7, 5.4 Hz, 1H), 3.13–2.46 (m, 2H); ^{13}C NMR (100 MHz, $CDCl_3$) δ 170.7, 148.1, 145.8, 139.5, 136.8, 133.6, 132.9, 130.8, 130.0, 129.1, 128.8, 128.1, 127.7, 126.8, 125.0, 124.6, 123.5, 115.6, 52.2, 49.4, 42.2; ESI-MS (positive): 409.1 $(M + 1)^+$.

*4.1.3.24. 2,3-Dihydro-2-(chlorophenyl)-5-(2-nitrobenzyl)-1,5-benzothiazepin-4(5H)-one (**6x**).* Yield: 88%; mp 164.8–167.4 °C; ^{1}H NMR (400 MHz, $CDCl_3$) δ 8.29–6.77 (m, 12H), 5.53 (q, J = 17.2 Hz, 2H), 4.85 (dd, J = 12.7, 5.4 Hz, 1H), 3.15–2.69 (m, 2H); ^{13}C NMR (100 MHz, $CDCl_3$) δ 170.6, 148.1, 145.8, 142.1, 136.8, 133.6, 132.6, 130.9, 129.6, 129.0, 128.1, 127.5, 127.4, 126.7, 125.0, 123.5, 52.2, 49.4, 41.9; ESI-MS (positive): 425.0 $(M + 1)^+$.

*4.1.3.25. 2,3-Dihydro-2-(bromophenyl)-5-(2-nitrobenzyl)-1,5-benzothiazepin-4(5H)-one (**6y**).* Yield: 93%; mp 178.0–181.5 °C; ^{1}H NMR (400 MHz, $CDCl_3$) δ 8.38–6.78 (m, 12H), 5.53 (q, J = 17.2 Hz, 2H), 4.84 (dd, J = 12.7, 5.3 Hz, 1H), 3.29–2.60 (m, 2H); ^{13}C NMR (100 MHz, $CDCl_3$) δ 170.6, 148.1, 145.8, 142.1, 136.8, 133.6, 132.6, 130.9, 129.6, 129.0, 128.1, 127.5, 127.4, 126.7, 125.0, 123.5, 52.2, 49.4, 41.9; ESI-MS (positive): 469.0, 471.0 $(M + 1)^+$.

4.2. Biological evaluation

Human recombinant glycogen synthase kinase-3β (catalog number 14–306) was purchased from Millipore Corporation (Dundee, UK). The prephosphorylated polypeptide substrate GS-2 was synthesized by GL Biochem Ltd (Shanghai, China). Kinase-Glo Luminescent Kinase Assay (catalog number V6713) was obtained from Promega Corporation (Madison, WI). ATP·2Na was purchased from Roche. TDZD-8 (catalog number 098K4602V) was supplied by Sigma–Aldrich (St. Louis, MO). Assay buffer contained 50 mM HEPES (pH 7.5), 1 mM EDTA, 1 mM EGTA, and 15 mM magnesium acetate. Glow-type luminescence was recorded by Fluoroskan Ascent Fl (Thermo Electron, US).

4.2.1. Inhibition of GSK-3β

The measurement of GSK-3β inhibition was performed in assay buffer using black 96-well plates according to the Kinase-Glo assay method of Baki [20]. In a typical assay, 4 μL of interest compound with different concentration (dissolved in DMSO) was diluted by 14 μL of assay buffer, and 2 μL (20 ng) of enzyme solution were added to each well followed by 20 μL of assay buffer containing 12.5 μM substrate and 4 μM ATP. After 30 min of incubation at 30 °C, the enzymatic reaction was stopped with 40 μL of Kinase-Glo reagent. Glow-type luminescence was recorded after 10 min. The activity is proportional to the difference of the total and consumed ATP. The inhibitory activities were calculated on the basis of maximal activities measured in the absence of inhibitor. The IC_{50} value was defined as the concentration of each compound that reduces 50% the enzymatic activity with respect to that without inhibitors.

4.2.2. Kinetic analysis on GSK-3β

The protocol of the whole kinetic experiments was much similar to the one of GSK-3β inhibition tests. The activities of compound **6v** were measured separately at its two different concentrations as 25 μM and 50 μM. In the experiments for testing the relationship between **6v** and ATP, the concentration of substrate GS-2 was kept unchanged at 6.25 μM, while the concentration of ATP was set at 0.5 μM, 1 μM, 2 μM, 4 μM and 8 μM separately. Then, in the following experiments for testing the relationship between **6v** and GS-2, the concentration of ATP was kept unchanged at 2 μM while GS-2 concentration was set at 0.78 μM, 1.56 μM, 3.13 μM, 6.25 μM and 12.5 μM separately. Double-reciprocal plotting of the data was depicted in Fig. 3.

Reversibility of compound **6v** was determined by evaluating its activity to the enzyme at different incubation time. The incubation time was set at 0 min, 5 min and 10 min while concentration of compound **6v** was kept unchanged at 12.5 μM and 25 μM separately. The inhibition effects of compound **6v** in these conditions were shown in Fig. 3C.

4.2.3. Selectivity studies of tyrosine kinases inhibition

The experimental procedures for the inhibition of nine tyrosine kinases were conducted using ELISA method reported by Geng et al. [30]. 20 μg/ml of Poly (Glu, Tyr) 4:1 (Sigma) was pre-coated as a substrate in 96-well plates. 50 μL of 10 μM ATP solution diluted with kinase reaction buffer (50 mM HEPES pH 7.4, 50 mM $MgCl_2$, 0.5 mM $MnCl_2$, 0.2 mM Na_3VO_4 and 1 mM DTT) was added to each well. Various concentrations of compounds diluted in 10 μL of 1% DMSO (v/v) were added to each reaction well, with 1% DMSO (v/v) used as the negative control. The kinase reaction was initiated by the addition of purified tyrosine kinase proteins diluted with 40 μL of kinase reaction buffer solution. After incubation for 60 min at 37 °C, the plate was washed three times with Phosphate Buffered Saline (PBS) containing 0.1% Tween 20 (T-PBS). Next, 100 μL of anti-phospho tyrosine (PY99) antibody (1:500 diluted in 5 mg/mL BSA T-PBS) was added. After 30 min incubation at 37 °C, the plate was washed three times. A solution of 100 μL of horseradish peroxidase-conjugated goat anti-mouse IgG (1:2000 diluted in 5 mg/mL BSA T-PBS) was added. The plate was reincubated at 37 °C for 30 min, and

washed as before. Finally, 100 μL of a solution containing 0.03% H_2O_2 and 2 mg/mL *o*-phenylenediamine in 0.1 mM citrate buffer, pH 5.5, was added and samples were incubated at room temperature until color emerged. The reaction was terminated by the addition of 50 μL of 2 M H_2SO_4, and the plate was read using a multi well spectrophotometer (VERSA max™, Molecular Devices, Sunnyvale, CA, USA) at 490 nm. The inhibition rate (%) was calculated using the following equation: $[1-(A_{490}/A_{490\ \text{control}})] \times 100\%$.

4.3. Molecular modeling

The GSK-3β protein–ligand complex crystal structure (PDB ID: 1PYX) was chosen as the template for docking analysis, which was proceeded using GOLD 5.0 software. For ligand preparation, the structure of compound **6v** was generated and minimized using Sybyl 6.9 with the MMFF94 force field until a 0.01 kcal/mol gradient was reached. For enzyme preparation, the hydrogen atoms were added, and all of ligands, metal, water, and cocrystallized phosphates were removed. The binding site was defined as a sphere of 10 Å radius around the residue Arg 209. Docking calculations were performed with other parameters set in their default values. Top five scored docking complex were extracted for conformational cluster analysis in order to find the docking results with the highest probability.

Acknowledgments

We gratefully acknowledge the financial support by Specialized Research Fund for the Doctoral Program of Higher Education of China (Grant No. 20070246089), the Shanghai Committee of Science and Technology of China (Grant No.10ZR1401800), and National Drug Innovative Program (Grant No. 2009ZX09301-011). Thanks are due to Professor Jianzhong Lu (Department of Pharmaceutical Analysis, School of Pharmacy, Fudan University) and to Professor Meiyu Geng (Division of Antitumor Pharmacology, State Key Laboratory of Drug Research, Shanghai Institute of Materia Medica) for assistance with the bioassay and biological evaluation.

Appendix A. Supplementary data

Supplementary data related to this article can be found at http://dx.doi.org/10.1016/j.ejmech.2012.09.021.

References

[1] P. Cohen, D. Yellowlees, A. Aitken, A. Donella-Deana, B.A. Hemmings, P.J. Parker, Eur. J. Biochem. 124 (1982) 21–35.
[2] J.R. Woodgett, Sci. STKE 100 (2001) 12.
[3] E.M. Hur, F.Q. Zhou, Nat. Rev. Neurosci. 11 (2010) 539–551.
[4] A. Kannoji, S. Phukan, V. Sudher Babu, V.N. Balaji, Expert Opin. Ther. Targets 12 (2008) 1443–1455.
[5] D. Alonso, A. Martinez, Glycogen Synthase Kinase 3 (GSK-3) and Its Inhibitors, JohnWiley & Sons, Hoboken, NJ, USA, 2006, pp. 307–331.
[6] A. Martinez, C. Gil, D.I. Perez, Int. J. Alzheimer's Dis. 2011 (2011) 280502.
[7] A. Martinez, Med. Res. Rev. 28 (2008) 773–796.
[8] P. Bamborough, D. Drewry, G. Harper, G.K. Smith, K. Schneider, J. Med. Chem. 51 (2008) 7898–7914.
[9] H. Eldar-Finkelman, A. Licht-Murava, S. Pietrokovski, M. Eisenstein, Biochim. Biophys. Acta 1804 (2010) 598–603.
[10] A. Martinez, M. Alonso, A. Castro, C. Pérez, F.J. Moreno, J. Med. Chem. 45 (2002) 1292–1299.
[11] T. del Ser, Alzheimer's Dementia 6 (2010) S147.
[12] S. Conde, D.I. Pérez, A. Martínez, C. Perez, F.J. Moreno, J. Med. Chem. 46 (2003) 4631–4633.
[13] D.I. Perez, S. Conde, C. Pérez, C. Gil, D. Simon, F. Wandosell, F.J. Moreno, J.L. Gelpí, F.J. Luque, A. Martínez, Bioorg. Med. Chem. 17 (2009) 6914–6925.
[14] D.I. Perez, V. Palomo, C.P. rez, C. Gil, P.D. Dans, F.J. Luque, S. Conde, A. Martinez, J. Med. Chem. 54 (2011) 4042–4056.
[15] H. Eldar-Finkelman, M. Eisenstein, Curr. Pharm. Des. 15 (2009) 2463–2470.
[16] M. Hamann, D. Alonso, E. Martín-Aparicio, A. Fuertes, M.J. Pérez-Puerto, A. Castro, S. Morales, M.L. Navarro, M. del Monte-Millán, M. Medina, J. Nat. Prod. 70 (2007) 1397–1405.
[17] J.C. Lancelot, B. Letois, C. Saturnono, P. De Caprariis, M. Robba, Org. Prep. Proced. Int. 24 (1992) 204–208.
[18] A. Levai, H. Duddeck, Pharmazie 38 (1983) 827–828.
[19] S.F. Wnuk, S.M. Chowdhury, P.I. Garcia Jr., M.J. Robins, J. Org. Chem. 67 (2002) 1816–1819.
[20] A. Baki, A. Bielik, L. Molnar, G. Szendrei, G.M. Keseru, Assay Drug Dev. Technol. 5 (2007) 75–83.
[21] GOLD, Version 5.0, The Cambridge Crystallographic Data Centre, http://www.ccdc.cam.ac.uk.
[22] V. Palomo, I. Soteras, D.I. Perez, C. Perez, C. Gil, N.E. Campillo, A. Martinez, J. Med. Chem. 54 (2011) 8461–8470.
[23] Discovery Studio, Version 3.0, Accelrys Software Inc., http://www.accelrys.com.
[24] N. Lensen, S. Mouelhi, M. Bellassoued, Synth. Commun. 31 (2001) 1007–1011.
[25] M. Bellassoued, N. Lensen, M. Bakasse, S. Mouelhi, J. Org. Chem. 63 (1998) 8785–8789.
[26] J. Krapcho, E.R. Spitzmiller, C.F. Turk, J. Med. Chem. 6 (1963) 544–546.
[27] A.N. Nesmeyanov, L.I. Zakharkin, R. Kh Freidlina, Dokl. Akad. Nauk SSSR 111 (1956) 114–116.
[28] A. Lebedev, A. Lebedeva, V. Sheludyakov, E. Kovaleva, O. Ustinova, I. Kozhevnikov, Russ. J. Gen. Chem. 75 (2005) 1113–1124.
[29] P. Ghorai, A. Kraus, M. Keller, C. Gotte, P. Igel, E. Schneider, D. Schnell, G.n. Bernhardt, S. Dove, M. Zabel, S. Elz, R. Seifert, A. Buschauer, J. Med. Chem. 51 (2008) 7193–7204.
[30] Y. Wang, J. Ai, Y. Chen, L. Wang, G. Liu, M. Geng, A. Zhang, J. Med. Chem. 54 (2011) 2127–2142.
[31] Sybyl Version 6.9, Triops Inc, St. Louis, MO.